Polymer 49 (2008) 3335–3345

Contents lists available at ScienceDirect

Polymer

journal homepage: www.elsevier.com/locate/polymer

Effect of modified carbon nanotube on the properties of aromatic polyester nanocomposites

Jun Young Kim [a,*], Sang Il Han [a], Seungpyo Hong [b]

[a] Material Laboratory, Corporate R&D Center, Samsung SDI Co., Ltd., 575 Shin-dong, Yeongtong-gu, Suwon-si, Gyeonggi-do 443-731, Republic of Korea
[b] Department of Biopharmaceutical Sciences, University of Illinois, Chicago, IL 60612, USA

ARTICLE INFO

Article history:
Received 18 February 2008
Received in revised form 9 May 2008
Accepted 11 May 2008
Available online 22 May 2008

Keywords:
Carbon nanotube
Melt blending
Polymer nanocomposites

ABSTRACT

Aromatic polyester nanocomposites based on poly(ethylene 2,6-naphthalate) (PEN) and carbon nanotube (CNT) were prepared by melt blending using a twin-screw extruder. Modification of CNT to introduce carboxylic acid groups on the surface was performed to enhance intermolecular interactions between CNT and the PEN matrix through hydrogen bonding formation. Morphological observations revealed that the modified CNT was uniformly dispersed in the PEN matrix and increased interfacial adhesion between the nanotubes and the PEN, as compared to the untreated CNT. Furthermore, a very small quantity of the modified CNT substantially improved thermal stability and tensile strength/modulus of the PEN nanocomposites. This study demonstrates that the thermal, mechanical, and rheological properties of the PEN nanocomposites are strongly dependent on the uniform dispersion of CNT and the interactions between CNT and PEN, which can be enhanced by slight chemical modification of CNT, providing a design guide of CNT-reinforced PEN nanocomposites with a great potential for industrial uses.

1. Introduction

Carbon nanotubes (CNTs) have attracted a great deal of scientific interest as advanced materials for next generation since they were first reported by Iijima [1]. In particular, excellent mechanical strength, thermal conductivity, and electric current carrying ability of CNTs have created a high level of activity in materials research for potential applications such as hydrogen storage, lithium battery, fuel cell, filed emitting diode, gas sensor, and polymer nanocomposite [2–9]. Furthermore, a number of efforts have been made to develop high performance polymeric materials based on the CNTs, with the benefit of nanotechnology, in fields ranging from the basic science to the industrial applications [10–12]. However, because of their high cost and limited availability, only a few practical applications in industrial field such as electronic and electric appliances have been realized to date.

Poly(ethylene 2,6-naphthalate) (PEN) is a transparent aromatic polyester having a similar chemical structure to poly(ethylene terephthalate) (PET), a widely used polyester resin in conventional industry, with the exception that PEN has the naphthalene ring in the main chain instead of the benzene ring, and it is of great industrial importance because of its high performance, good physical properties, and low cost. As the introduction of the naphthalene ring into the main chains stiffens the polymer chains and improves their physical properties, PEN typically exhibits enhanced thermal, mechanical, and gas barrier properties as compared to PET. PEN thus holds a potential for industrial applications, including food packaging materials, high performance industrial fibers, magnetic recording tapes, and flexible printed circuits. In this regard, research and development have been extensively performed to date both to displace PET and to develop commercial applications of PEN, such a high performance polymer [13–21]. Although promising, however, insufficient mechanical properties and thermal stability of PEN have often hindered its practical application in a broad range of industry.

Polymer nanocomposites that are a new class of the materials based on the reinforcement of polymers using nanofillers have attracted a great deal of interest in fields ranging from the scientific to the industrial because of remarkable improvement in the physical and mechanical properties at low filler loadings. The CNTs are regarded as the promising reinforcements in the polymer nanocomposites due to the combination of their uniquely excellent properties with high aspect ratio and small size [10–12]. This feature has motivated considerable efforts to fabricate CNT/polymer nanocomposites, with the benefit of nanotechnology, in the development of advanced composite materials for next generation. For the fabrication of CNT/polymer nanocomposites, major goals to realize the potential applications of CNTs as nanoreinforcing fillers are (a) homogeneous dispersion of CNTs in the polymer matrix and (b) strong interfacial adhesion between CNT and polymer matrix

* Corresponding author. Tel.: +82 31 210 7103; fax: +82 31 210 7374.
E-mail address: junykim74@hanmail.net (J.Y. Kim).

0032-3861/$ – see front matter © 2008 Elsevier Ltd. All rights reserved.
doi:10.1016/j.polymer.2008.05.024

[22–24]. In general, CNT has a tendency to bundle together and to form some agglomeration because of intrinsic van der Waals attraction between the individual tubes [25]. Weak interfacial bonding between the nanotubes and the polymer matrix has limited the efficient load transfer to the polymer matrix, playing a limited reinforcement role in the polymer nanocomposites [26–28]. The functionalization of CNTs, which can be considered as an effective method to achieve the uniform dispersion of CNTs and their compatibility with the polymers, can lead to the enhancement of the interfacial adhesion between CNTs and polymer matrix, thereby improving the overall properties of CNT/polymer nanocomposites [29–33].

Currently, four processing techniques are in common use to fabricate CNT/polymer nanocomposites [34–41]: direct mixing, in situ polymerization, solution method, and melt compounding. Among these processing techniques, melt compounding has been accepted as the simplest and the most effective method from an industrial perspective, because this process makes it possible to fabricate high performance nanocomposites at low process cost, and facilitates commercial scale-up. Furthermore, the combination of a very small quantity of expensive CNT with conventional cheap thermoplastic polymers provides attractive possibilities for improving the physical properties of polymer nanocomposites using a cost-effective method.

In this study, aromatic polyester nanocomposites based on PEN and CNT were prepared by direct melt compounding in a twin-screw extruder to create high performance composite materials with low cost for possible practical applications in various industrial fields. In our previous works [42–44], we prepared the PEN nanocomposites reinforced with pristine CNT via direct melt compounding, and investigated the effects of pristine CNT on the nucleation and crystallization behavior, the rheological and mechanical properties, and the thermal stability and degradation kinetics of the PEN/CNT nanocomposites. In this study, pristine CNT was chemically modified to introduce functional groups on their surfaces for improving the dispersion of the nanotubes and the interfacial adhesion between the nanotubes and the polymer matrix, and the resultant nanocomposites were characterized by means of Fourier transform infrared (FT-IR) spectroscopy, Raman spectroscopy, X-ray photoelectron spectroscopy (XPS), differential scanning calorimetry (DSC), thermogravimetric analysis (TGA), scanning electron microscopy (SEM), and transmission electron microscopy (TEM) to clarify the effects of the pristine and modified CNTs on the structure and the properties of the PEN nanocomposites. In addition, the effects of pristine and modified CNTs on the rheological and mechanical properties of the polymer nanocomposites are discussed. Surface modification of the CNTs has provided remarkably enhanced physical properties of the resulting PEN-based nanocomposites. Our study suggests a simple and cost-effective method that will facilitate the industrial realization of the CNT-reinforced PEN nanocomposites with enhanced physical properties.

2. Experimental

2.1. Materials

Conventional thermoplastic polymer used was the PEN with an intrinsic viscosity of 0.97 dL/g, supplied by Hyo Sung Corp., Korea. The nanotube used was multi-walled CNT (degree of purity $> 95\%$) synthesized by a thermal chemical vapor deposition process, purchased from Iljin Nanotech Co., Korea. According to the supplier, their length and diameter were in the range of 10–50 and 10–30 nm, respectively, indicating that their aspect ratio reaches 1000. The concentrated sulfuric acid (H_2SO_4, 98%) and nitric acid (HNO_3, 68%) were purchased from the Sigma Aldrich Co., and they were used as-received without further purification.

2.2. Preparation of polymer nanocomposites

The CNT was modified by the following steps: the CNT was added to the mixture of concentrated H_2SO_4 and HNO_3 with a volumetric ratio of 3:1 and this mixture was sonicated at 80 °C for 4 h to create the carboxylic acid groups on the nanotube surface. After this mixture was cooled to room temperature, it was diluted with deionized water and then vacuum-filtered through 0.22 μm milipore PTFE membranes, and washed with an excess of distilled water until the pH value of the filtrate reached approximately 7. The filtrated solid was dried *in vacuo* at 70 °C for at least 24 h, yielding the modified CNT. The carboxylic acid groups were introduced in order to increase the CNT's chemical affinity with the PEN, yet to decrease the π–π stacking effect among the aromatic rings of the nanotubes, which often leads to the formation of their agglomeration [45]. Throughout the manuscript, the p-CNT and the m-CNT denote the pristine CNT and the modified CNT, respectively.

All the materials were dried at 120 °C *in vacuo* for at least 24 h before use, to minimize the effects of moisture. The PEN nanocomposites were prepared by a melt blending process in a Haake rheometer (Haake Technik GmbH, Germany) equipped with a twin-screw. The temperature of the heating zone, from the hopper to the die, was set to 280, 290, 295, and 285 °C, and the screw speed was fixed at 20 rpm. For the fabrication of the PEN nanocomposites, PEN was melt blended with the addition of CNT content, specified as 0.1 and 0.5 wt% in the polymer matrix. Upon completion of melt blending, the extruded strands were allowed to cool in the water-bath, and then cut into pellets with constant diameter and length using a rate-controlled PP1 pelletizer (Haake Technik GmbH, Germany).

2.3. Characterizations

The chemical structures of p-CNT and m-CNT were characterized by means of FT-IR measurement using a Magna-IR 550 spectrometer (Nicolet Co.) in the range 400–4000 cm^{-1} at room temperature. FT-IR spectra were obtained using a spectral resolution of 4 cm^{-1} and were averaged over 64 scans. The CNTs were mixed with KBr powder and then KBr discs were prepared using a die in a Carver press. The change in the structure of CNT by chemical modification was characterized by means of a JASCO NRS-3100 Raman spectrometer (JASCO Inc.) equipped with a 532 nm diode laser, and the laser beam with a nominal power of 30 mW was focused to a spot size of 5 μm diameter. The XPS spectra was obtained on a VG ESCALAB 220-I system using MgKα X-ray radiation as the excitation source with a pass energy of 1253.6 eV. The XPS analysis was performed under high vacuum conditions (10^{-9} Torr). All binding energies were referenced to the C_{1s} neutral carbon peak at 284.6 eV.

Thermal behavior of PEN/CNT nanocomposites were measured with a TA instrument 2010 DSC over the temperature range of 30–295 °C at a scanning rate of 10 °C/min under N_2 atmosphere. The samples with a typical mass of 6.5 ± 0.3 mg were encapsulated in sealed aluminum pans. The samples were first heated to 295 °C at a heating rate of 10 °C/min, maintained at that temperature for 10 min to eliminate any previous thermal history, and then cooled to room temperature at a cooling rate of 10 °C/min. Thermogravimetric analysis of PEN/CNT nanocomposites were performed with a TA instrument SDF-2960 TGA over the temperature range of 30–850 °C at a heating rate of 10 °C/min under nitrogen.

The rheological properties of PEN/CNT nanocomposites were performed on an ARES (Advanced Rheometric Expansion System) rheometer (Rheometric Scientific Inc.) in oscillation mode with the

parallel-plate geometry using the plate diameter of 25 mm and the plate gap setting of ~1 mm at 295 °C, by applying a time-dependent strain, $\gamma(t) = \gamma_0 \sin(\omega t)$ and measuring resultant shear stress, $\gamma(t) = \gamma_0[G' \sin(\omega t) + G'' \cos(\omega t)]$, where G' and G'' are storage and loss moduli, respectively. The frequency ranges were varied between 0.05 and 450 rad/s, and the strain amplitude was applied to be within the linear viscoelastic ranges.

The morphology of the PEN nanocomposites was observed using a JEOL 2000-FX TEM imaging microtomed ultrathin slices of the PEN nanocomposite films with an accelerating voltage of 120 kV. SEM experiments were conducted using a JEOL 6340 SEM with an accelerating voltage of 15 kV. The samples used for SEM observation were gold-coated *in vacuo* using ion sputtering before scanning to prevent charging in the electron beam. The mechanical properties of the PEN nanocomposites were measured at room temperature using an Instron 4465 testing machine, according to the procedures in the ASTM D 638 standard. The gauge length and the crosshead speed were set to 20 mm and 5 mm/min, respectively. The films of testing samples were prepared in a hydrolytic press at 295 °C, and they were conditioned at approximately 50% relative humidity for 24 h before the measurements. At least five measurements were performed for each sample and the results were averaged to obtain a mean value.

3. Results and discussion

3.1. Effect of CNT modification

The FT-IR spectra of the p-CNT and the m-CNT are shown in Fig. 1(a). The broad shoulder peak ranged in 3200–3400 cm^{-1} was attributed to the O–H stretching band induced by the hydroxyl groups attached at the CNT. The characteristic peak observed at approximately 1570 cm^{-1} was attributed to the IR-phonon mode of the multi-walled CNT [46,47]. For the m-CNT, the peaks observed at near 1190 and 1730 cm^{-1} were assigned to the C=O and C–O stretching vibrations of the carboxylic acid groups [47,48]. This result demonstrates that carboxylic acid groups on the surface of m-CNT were effectively induced via the chemical treatment. Thus, it is expected that the functional groups formed on the surface of the m-CNT contribute to the enhancement of the interaction in the PEN/m-CNT nanocomposites through hydrogen bonding formation, as shown in Scheme 1.

The Raman spectra of the p-CNT and the m-CNT are shown in Fig. 1(b). Similar patterns observed in the Raman spectra of the p-CNT and the m-CNT indicated that the chemical modification did not affect the graphite structure of the CNTs. It is known that this chemical modification of the CNTs in the HNO_3/H_2SO_4 mixture can be used to produce carboxylic acid groups at local defect sites on CNT and their ends [29]. The Raman spectra of the p-CNT and the m-CNT exhibited three characteristic peaks observed at near 1350, 1570, and 2690 cm^{-1}, respectively, which were termed D-band, G-band, and D^*-band (overtone of D-band), respectively [49]. The G-band, corresponding to the Raman-allowed phonon high-frequency mode, was related to the structural intensity of the sp^2-hybridized carbon atoms of the CNTs [50,51]. The D-band reflected the disorder-induced carbon atoms, resulting from the defects in the CNT and their ends, and its intensity decreases with the degree of the graphitization of the CNT [50,51]. As shown in Fig. 1(b), the relative intensity of D-band was slightly increased in the m-CNT, indicating that the sp^2 hybrid decreased and the sp^3 hybrid increased after the chemical modification of the p-CNT. In addition, the relative intensity ratio of G-band to D-band (I_G/I_D) of the m-CNT was slightly decreased compared to that of the p-CNT, which was attributed to the increase in the degree of disorder and the presence of the defects on the surface of the m-CNT by chemical modification [52]. The representative

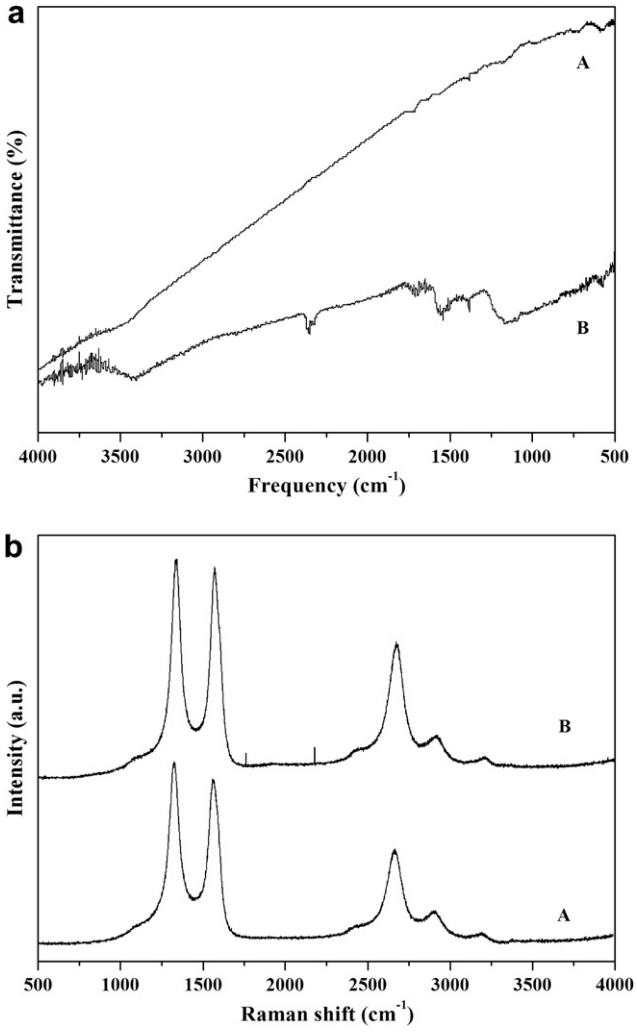

Fig. 1. (a) FT-IR and (b) Raman spectra of CNTs (A: p-CNT and B: m-CNT).

TEM images of the m-CNT are shown in Fig. 2. The m-CNT exhibited loosely entangled organization instead of showing the agglomerated structures or bundles observed in the p-CNT, implying more effective enhancement of the dispersion of the m-CNT than that of the p-CNT. However, it was reported that there was a possibility to occur the slight damage and the decreased

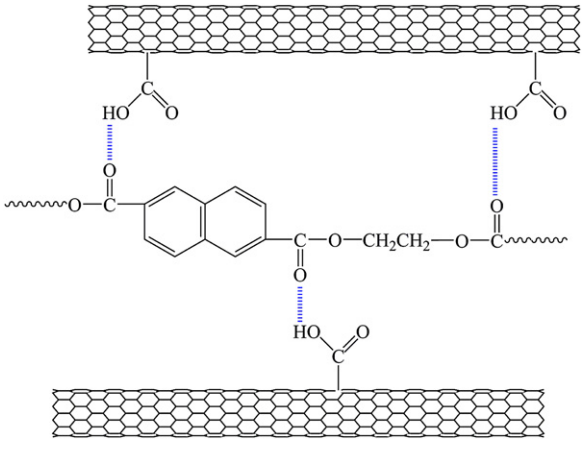

Scheme 1. Schematic showing possible interaction of hydrogen bonding between the m-CNT and the PEN matrix.

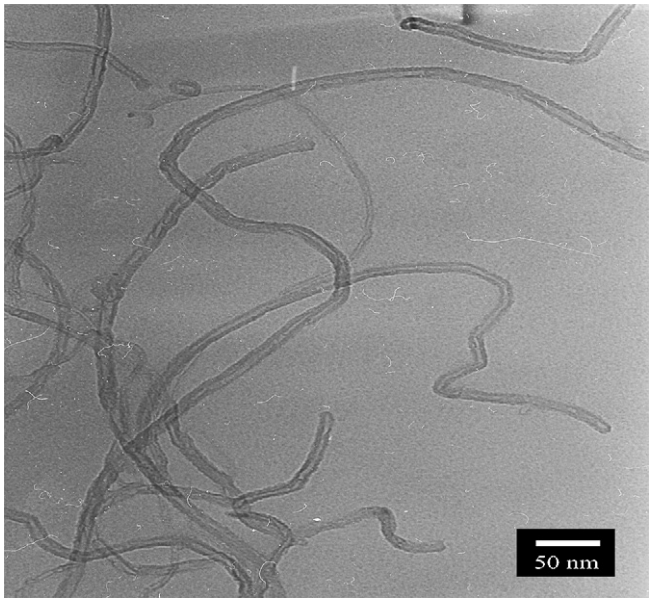

Fig. 2. Representative TEM images of the m-CNT after modification.

length in the nanotube structure induced by the strong acid treatment [53,54].

The elemental compositions of the PEN nanocomposites were characterized by XPS. The XPS survey spectra of pure PEN and the PEN/m-CNT nanocomposites are shown in Fig. 3. Two characteristic peaks corresponding to C_{1s} and O_{1s} at approximately 285 and 532 eV, respectively, were observed, which were assigned to the sp^2 carbon and the ether-type group with oxygen bonded to carbon [55,56]. The high resolution C_{1s} XPS spectra of pure PEN and the PEN/m-CNT nanocomposites are shown in Fig. 3(b and c). The C_{1s} spectra of pure PEN exhibited three characteristic peaks at 285, 286.5, and 288.7 eV, corresponding to C–C, C–O, and C═O groups, respectively [57]. Compared with that of pure PEN, the C_{1s} spectra of the PEN/m-CNT nanocomposites shift to higher binding energy, and also revealed the presence of three peaks, corresponding to C–C (285.2 eV), C–O (289.1 eV), and C═O (291.3 eV) groups, respectively. This slight shifting of the characteristic peaks to higher binding energy for the PEN/m-CNT nanocomposites was attributed to the interaction of functional groups formed on the surface of m-CNT with the PEN molecules as well as good dispersion of the m-CNT in the PEN matrix [24].

3.2. Thermal behavior

TGA was conducted to identify the thermal stability of the p-CNT, the m-CNT, and the PEN nanocomposites, and their results are shown in Fig. 4. For the m-CNT, the first weight loss observed below 100 °C in the TGA traces was attributed to the loss of water molecules in the nanocomposite samples [58]. In addition, the further gradual decrease in the residual weight was attributed to organic decomposition of thermally unstable functional groups formed on the surface of the m-CNT [59]. As shown in Fig. 4(b), the incorporation of the p-CNT and the m-CNT into the PEN matrix can increase the thermal degradation temperatures and the residual yields of the PEN nanocomposites and this enhancing effect was more significant in the PEN/m-CNT nanocomposites. This result indicated that the presence of the p-CNT and m-CNT could lead to the stabilization of the PEN matrix, resulting in the enhancement of the thermal stability of the PEN nanocomposites. The CNTs can effectively act as physical barriers to prevent the transport of volatile decomposed products out of the PEN nanocomposites during

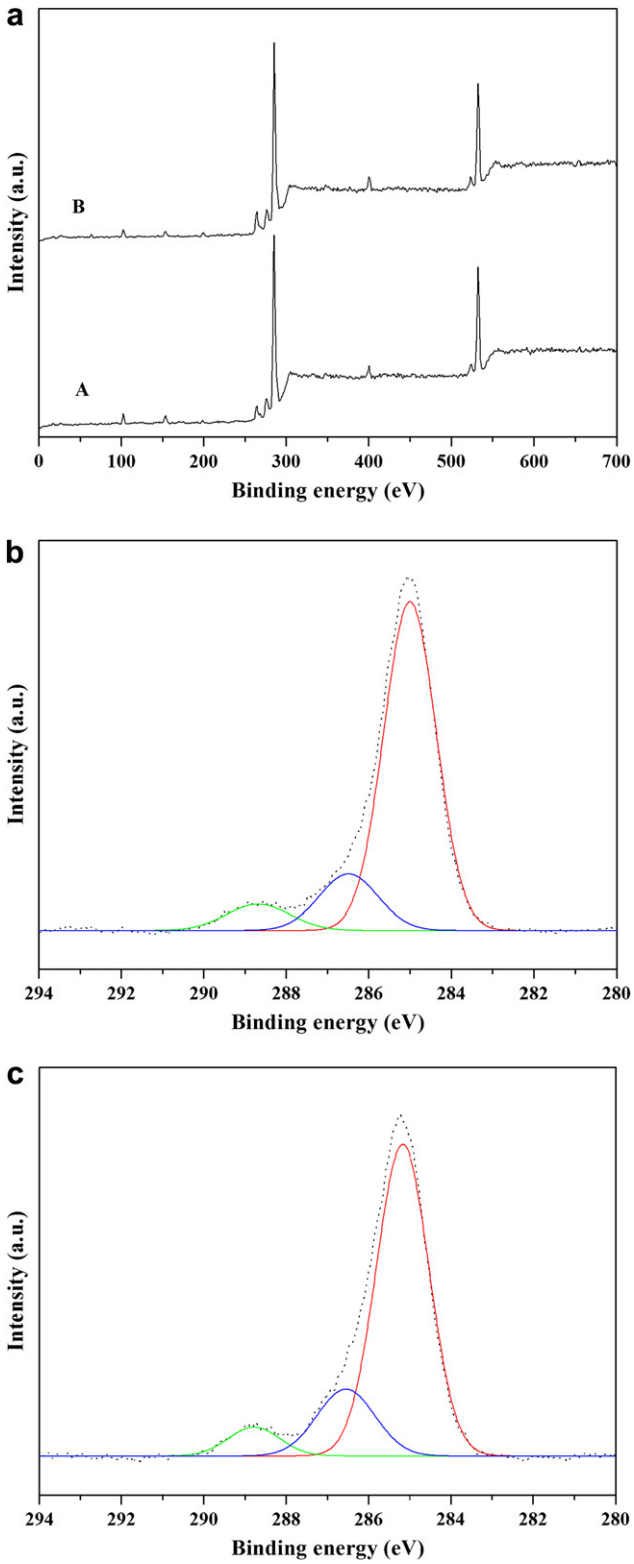

Fig. 3. (a) XPS survey spectra of PEN nanocomposites (A: PEN and B: PEN/m-CNT) and high resolution C_{1s} XPS spectra of (b) PEN and (c) PEN/m-CNT nanocomposites.

thermal decomposition. In addition, good interfacial adhesion between the m-CNT and the PEN matrix may restrict the thermal motion of the PEN molecules [60], resulting in further improvement in the thermal stability of the PEN/m-CNT nanocomposites.

The TGA kinetic analysis was conducted on the PEN nanocomposites to clarify the effects of the p-CNT and the m-CNT on the

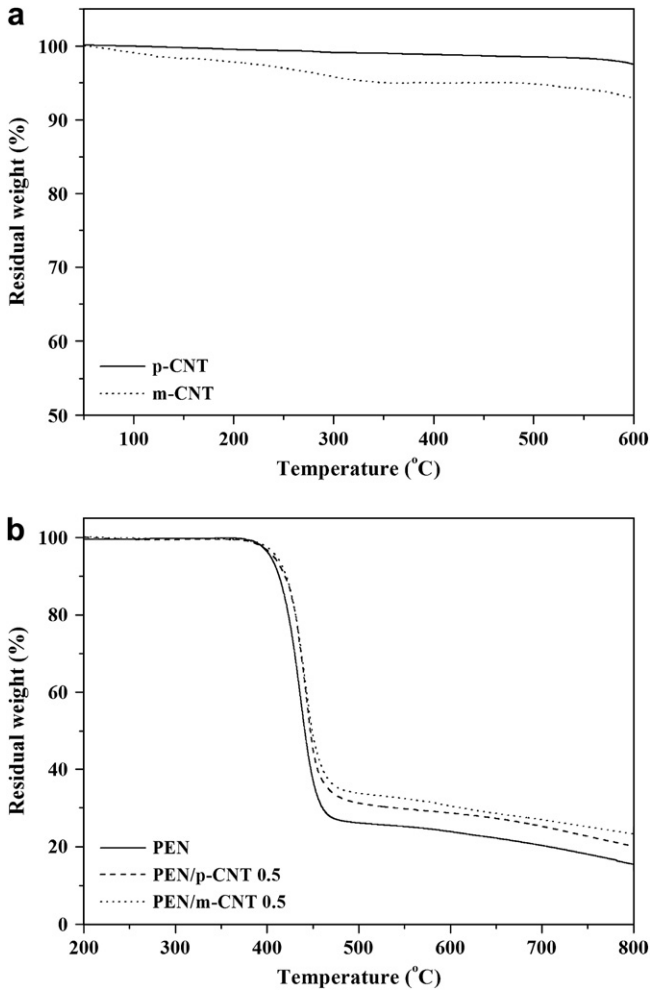

Fig. 4. TGA thermograms of (a) the p-CNT and the m-CNT and (b) the PEN nanocomposites.

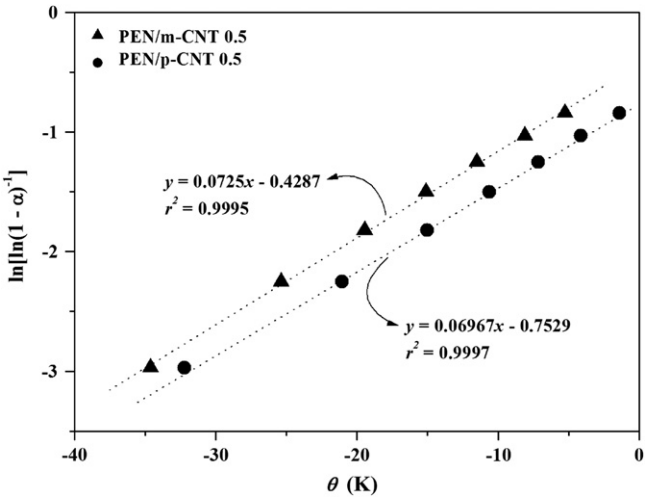

Fig. 5. Plots of $\ln[\ln(1-\alpha)^{-1}]$ versus θ as shown for PEN/p-CNT and PEN/m-CNT nanocomposites.

thermal stability of the PEN nanocomposites. The thermal decomposition temperatures and decomposition kinetic parameters such as the initial decomposition temperature, the integral procedure temperature, the temperature at maximum rate of weight loss (T_{dm}), and the activation energy for decomposition (E_a) are in common use to estimate the thermal stability of polymers or polymer nanocomposites. The activation energy for the thermal decomposition (E_a) of the PEN nanocomposites can be estimated from the TGA thermograms by the Horowitz–Metzger integral kinetic method [61] as follows:

$$\ln\left[\ln(1-\alpha)^{-1}\right] = \frac{E_a\theta}{RT_{dm}^2} \quad (1)$$

where α is the weight loss; E_a is the activation energy for the thermal decomposition; T_{dm} is the temperature at the maximum rate of weight loss; θ is the variable auxiliary temperature defined as $\theta = T - T_{dm}$; and R is the universal gas constant. The activation energy (E_a) can be determined from the slope of the plot of $\ln[\ln(1-\alpha)^{-1}]$ versus θ as shown in Fig. 5. The E_a values of the PEN nanocomposites containing the p-CNT and the m-CNT were 293.5 and 305.3 kJ/mol, respectively. Compared with the PEN/p-CNT nanocomposites, the higher E_a value of the PEN/m-CNT nanocomposites suggested that the PEN/m-CNT nanocomposites with more uniform dispersion of the m-CNT were more thermally stable than the PEN/p-CNT nanocomposites. This feature was also attributed to the interactions between the m-CNT and the PEN matrix, which increase the activation of the thermal decomposition of the PEN matrix relative to the p-CNT. Similar observation has reported that in the case of single-walled carbon nanotube (SWNT) and polyisoprene (PI) nanocomposites, the improved thermal stability and increased weight loss of functionalized SWNT/PI nanocomposite may be associated with the enhanced interactions between the PI and the organically modified SWNT side walls [62]. Because of excellent thermal conductivity of CNT [63,64], the enhanced interfacial interaction between the m-CNT and the PEN matrix resulted in the increased thermal conductivity of the PEN nanocomposites, leading to the improvement in the thermal stability. In addition, it can be deduced that the E_a values of the PEN nanocomposites calculated from the Horowitz–Metzger method exhibited good reliance on describing the thermal decomposition kinetics of the PEN nanocomposites, which was confirmed by the fact that the values of the correlation coefficient (r^2) were greater than 0.99.

The DSC thermograms of the PEN nanocomposites are shown in Fig. 6. The incorporation of the p-CNT has little effect on the glass transition temperature (T_g) and melting temperature (T_m) of the PEN nanocomposites. However, the T_g of the PEN/m-CNT nanocomposites slightly increased with the introduction of the m-CNT. The increase in the T_g of the PEN/m-CNT nanocomposites was attributed to the hindrance of the segmental motion of the PEN macromolecular chains with the presence of the m-CNT [65]. In addition, the crystallization temperatures were significantly increased with the introduction of the p-CNT and the m-CNT, indicating the efficiency of them as strong nucleating agents for the crystallization of PEN. This result suggested the enhancement of the crystallization of the PEN nanocomposites with the presence of the p-CNT and the m-CNT. For CNT-filled polymer nanocomposites, the accelerated crystallizations by the presence of CNTs through heterogeneous nucleation have been also reported [44,66,67].

3.3. Rheological properties

The complex viscosities ($|\eta^*|$) of the PEN nanocomposites as a function of frequency are shown in Fig. 7. The complex viscosities of pure PEN and the PEN nanocomposites were decreased with increasing frequency, indicating a non-Newtonian behavior over the whole frequency range measured. The shear thinning behavior observed in the PEN nanocomposites was attributed to the random orientation and entangled molecular chains in the nanocomposites during the applied shear force. The PEN nanocomposites containing

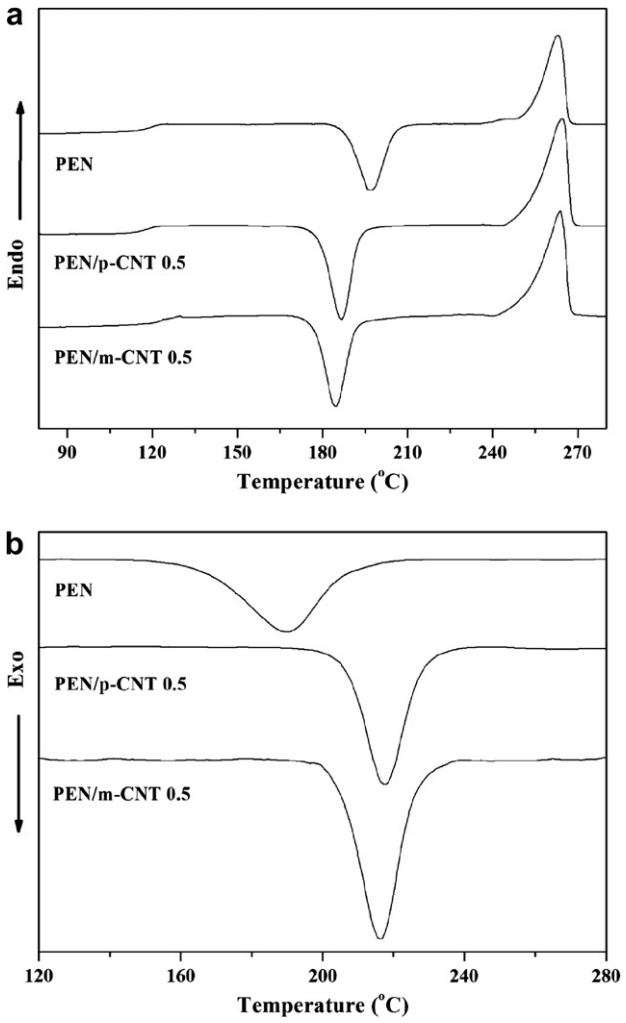

Fig. 6. DSC of (a) heating and (b) cooling traces of PEN nanocomposites.

the p-CNT and the m-CNT nanocomposites exhibited higher $|\eta^*|$ value than that of pure PEN at low frequency, indicating that the interconnected or network structures formed as a result of particle–particle and particle–polymer interactions. In addition, the PEN nanocomposites exhibited shear thinning behavior, resulting from the break down of these structures with increasing frequency. The $|\eta^*|$ of the PEN nanocomposites containing the m-CNT was further increased due to the increase in the interactions between the PEN and the nanotubes. Furthermore, the PEN/m-CNT nanocomposites exhibited higher $|\eta^*|$ and more distinct shear thinning behavior over the whole frequency range, relative to the other systems, suggesting either better dispersion of the nanotubes or stronger nanotube–polymer interactions. It was reported that the higher viscosity and more distinct shear thinning behavior were indicative of stronger interfacial interactions in the CNT and epoxy nanocomposite systems with more uniform dispersion of the CNT [68]. The increase in the $|\eta^*|$ of the PEN nanocomposites was closely related to the increase in the storage modulus, which will be described in the following section.

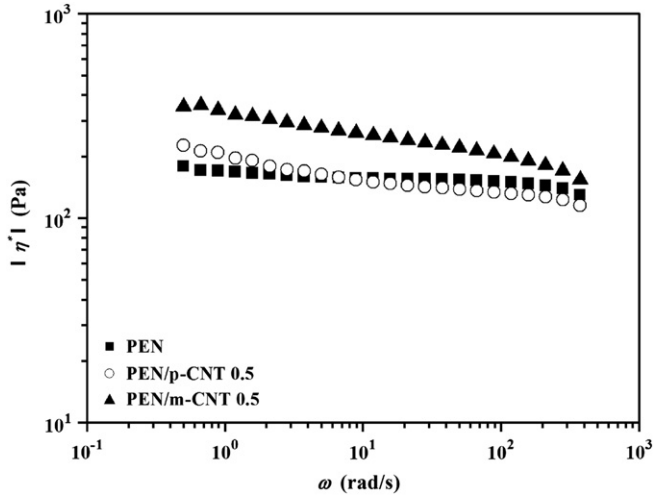

Fig. 7. Variations of complex viscosity of PEN nanocomposites as a function of frequency.

The shear thinning exponent (n) for the PEN nanocomposites can be obtained from the relationship of $|\eta^*| \approx \omega^n$ [69], and their results are summarized in Table 1. This result indicated that shear thinning behavior of the PEN nanocomposites significantly depended on the presence of the p-CNT and the m-CNT. The n values of the PEN nanocomposites slightly decreased with the introduction of the p-CNT and the m-CNT and this effect was more pronounced in the case of the m-CNT. This phenomenon was attributed to the enhancement of the interfacial interactions between the m-CNT and the PEN matrix as well as the uniform dispersion of the m-CNT. Pinnavaia and Beall [70] suggested that the better the nanofillers are dispersed, the stronger is the reinforcing effect on the polymer nanocomposites at a given filler content. As shown in Table 1, the PEN/p-CNT and the PEN/m-CNT nanocomposites exhibited slightly different n values even at the same CNT content, indicating the influence of the modification on the extent of CNT dispersion. In addition, it can be observed that the PEN nanocomposites containing the p-CNT and the m-CNT show the relationship between the shear thinning exponent and the mechanical properties for the PEN nanocomposites: the more the shear thinning behavior, the better the reinforcement effect on the mechanical properties. Similar observation has been reported in that the tensile modulus of the modified clay/poly(butylene terephthalate) nanocomposites prepared via melt compounding was improved with lower values of the shear exponent [71]. This result will be described in the following discussion of the mechanical properties of the PEN nanocomposites.

The storage modulus (G') and loss modulus (G'') of the PEN nanocomposites with the applied frequency are shown in Fig. 8. The values of G' and G'' for the PEN nanocomposites increased with increasing frequency and this enhancing effect was more significant at low-frequency region. This rheological response is similar to the relaxation behavior of the typical filled-polymer composite systems [72,73]. If the polymer chains are fully relaxed and exhibit a characteristic homopolymer-like terminal behavior, the flow curves of polymers can be expressed by a power law of $G' \propto \omega^2$ and $G'' \propto \omega$ [74]. Krisnamoorti and Giannelis [75] reported that the slopes of $G'(\omega)$ and $G''(\omega)$ for the polymer/layered silicate nanocomposites were much smaller than 2 and 1, respectively, suggesting that large deviations in the presence of a small quantity of layered silicate were caused by the formation of a network-like structures in the molten state. The slopes of the terminal zone of G' and G'' for the PEN nanocomposites are presented in Table 1. This

Table 1
Variations of low-frequency slopes of $|\eta^*|$, G', and G'' versus ω for the PEN nanocomposites

Materials	Slope of $\|\eta^*\|$ versus ω	Slope of G' versus ω	Slope of G'' versus ω
PEN	−0.13	1.26	0.95
PEN/p-CNT 0.5	−0.17	1.02	0.89
PEN/m-CNT 0.5	−0.19	0.93	0.85

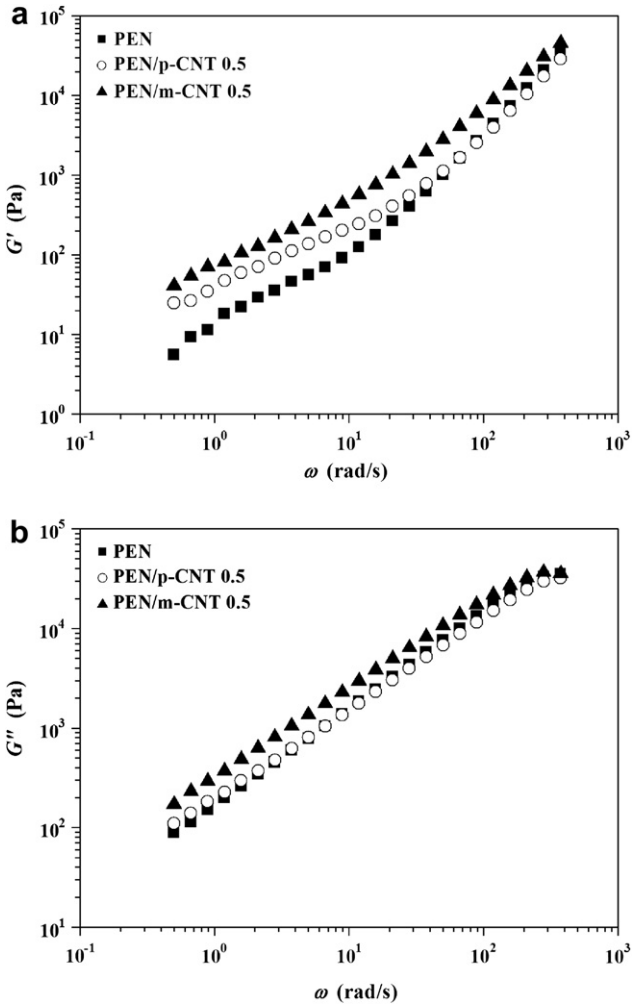

Fig. 8. (a) Storage modulus (G') and (b) loss modulus (G'') of PEN nanocomposites as a function of frequency.

result indicated the non-terminal behavior with the power-law dependence for G' and G'' of the PEN nanocomposites. Similar non-terminal low-frequency rheological behavior has been observed in ordered block copolymers and smectic liquid–crystalline small molecules [76,77]. The decrease in the slope of G' and G'' for the PEN nanocomposites with the introduction of the nanotubes was explained by the fact that the nanotube–nanotube or the nanotube–polymer interactions can lead to the formation of the interconnected or network-like structures, resulting in the pseudo solid-like behavior of the PEN nanocomposites.

As shown in Fig. 8, the extent of the increase in G' of the PEN nanocomposites was higher than that of G'' over the frequency range measured. The values of G' and G'' for the PEN nanocomposites were higher than those of pure PEN, particularly at low frequency, and this enhancing effect was more pronounced in the case of the m-CNT. The higher G' and G'' values of the PEN nanocomposites at low frequency demonstrated the formation of the interconnected or network structures via particle–particle and particle–polymer interactions by the presence of the nanotubes, resulting in more elasticity than pure PEN. As the applied frequency increased, the interconnected or network structures were broken down due to high levels of shear force and the PEN nanocomposites exhibited almost similar or slightly higher G' and G'' values than that of pure PEN at high frequency. Furthermore, the values of G' and G'' for the PEN/m-CNT nanocomposites were higher than those of pure PEN and the PEN/p-CNT nanocomposites over the whole

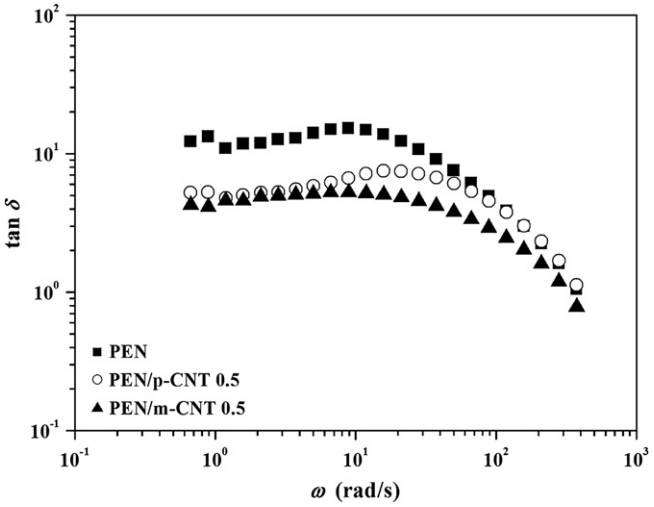

Fig. 9. Variation of tan δ as a function of frequency for PEN nanocomposites.

frequency range measured, suggesting the increase in the interactions between the m-CNT and the PEN matrix.

The variation of tan δ with frequency for the PEN nanocomposite is shown in Fig. 9. Shear deformation can lead to the partial orientation of the molecules in polymer chains, resulting in the decrease in tan δ of the PEN nanocomposites with increasing frequency. It can be observed that the loss tangent maximum of the PEN nanocomposites shifted to higher frequency with the introduction of the p-CNT and the m-CNT, implying the formation of the interconnected or network structures in the polymer nanocomposites [43]. The plots of the phase angle (δ) versus the absolute value of the complex modulus ($|G^*|$) for the PEN nanocomposites, which is known as the Van Gulp–Palmen plot [78–80], are shown in Fig. 10. The decrease in the phase angle with decreasing the complex modulus indicated the enhancement of the elastic behavior. The PEN nanocomposites containing the p-CNT and the m-CNT exhibited smaller δ values at lower $|G^*|$ values, indicating that the incorporation of the nanotube enhanced the elastic behavior of the PEN nanocomposites and this enhancing effect was more pronounced in the case of the m-CNT.

As described in the previous sections, the values of G' and G'' for the PEN nanocomposites containing the p-CNT and the m-CNT were higher than that of pure PEN and this enhancing effect was

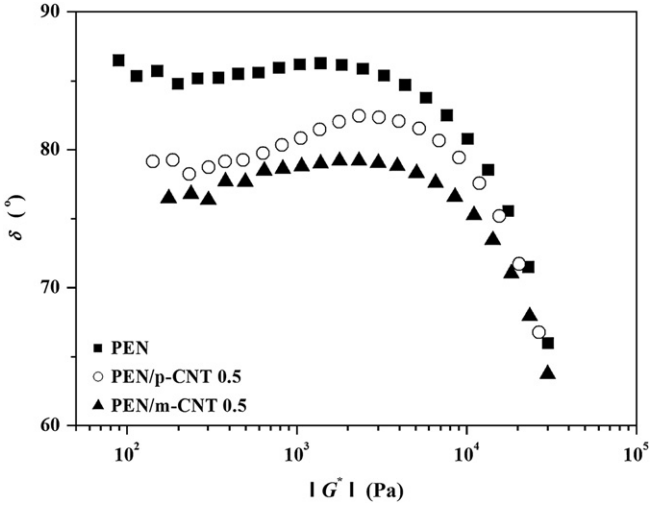

Fig. 10. Plots of phase angle versus complex modulus of PEN nanocomposites.

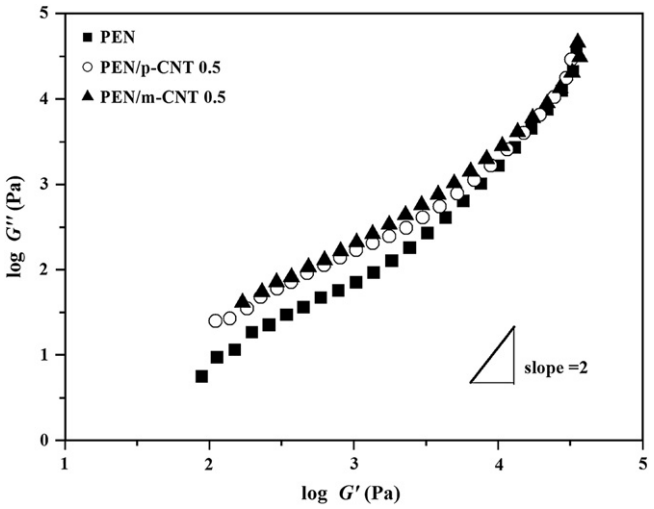

Fig. 11. Plots of log G' versus log G'' for PEN nanocomposites.

more significant in the case of the PEN/m-CNT nanocomposites. The plot of log G' versus log G'' for the PEN nanocomposites is shown in Fig. 11. In general, the Cole–Cole plot provides a master curve with a slope of 2 for isotropic and homogeneous polymer melts, irrespective of temperatures [81]. The PEN nanocomposites did not provide a perfect single master curve, and exhibited the shifting and the change of the slope of the plot with the introduction of the p-CNT and the m-CNT. The slopes in the terminal regime of the PEN nanocomposites were less than 2, indicating that the PEN nanocomposite systems were heterogeneous and they underwent some chain conformational changes due to the interconnected or network structures by the presence of the nanotubes. In addition, the slope of the PEN/m-CNT nanocomposites was lower than that of the PEN/p-CNT nanocomposites. This phenomenon may be attributed to the existence of the interfacial interactions between the m-CNT and the PEN matrix. However, over the G'' values of approximately 10^4, the slope of PEN nanocomposites increased and approached to similar slope of pure PEN, indicating that the interconnected or network structures formed by the nanotube–nanotube and the polymer–nanotube interactions were collapsed by high levels of shear force.

3.4. Morphology

The m-CNT exhibited less entangled structures due to the functional groups formed on their surfaces via chemical modification compared with the p-CNT showing more aggregated structures. The representative TEM images of the PEN/m-CNT 0.1 nanocomposites are shown in Fig. 12(a). In general, the drawbacks related to the homogeneous dispersion of the nanotubes in the polymer matrix resulted from intrinsic van der Waals attractions between the individual nanotubes in combination with high aspect ratio and large surface area, making it difficult for the nanotubes to disperse in the polymer matrix. The interfacial adhesion between the nanotubes and the polymer matrix plays an important role in improving the properties of the polymer nanocomposites. As shown in Fig. 12(a) and (b), the m-CNT was dispersed well in the PEN nanocomposites, which was explained by the fact that the m-

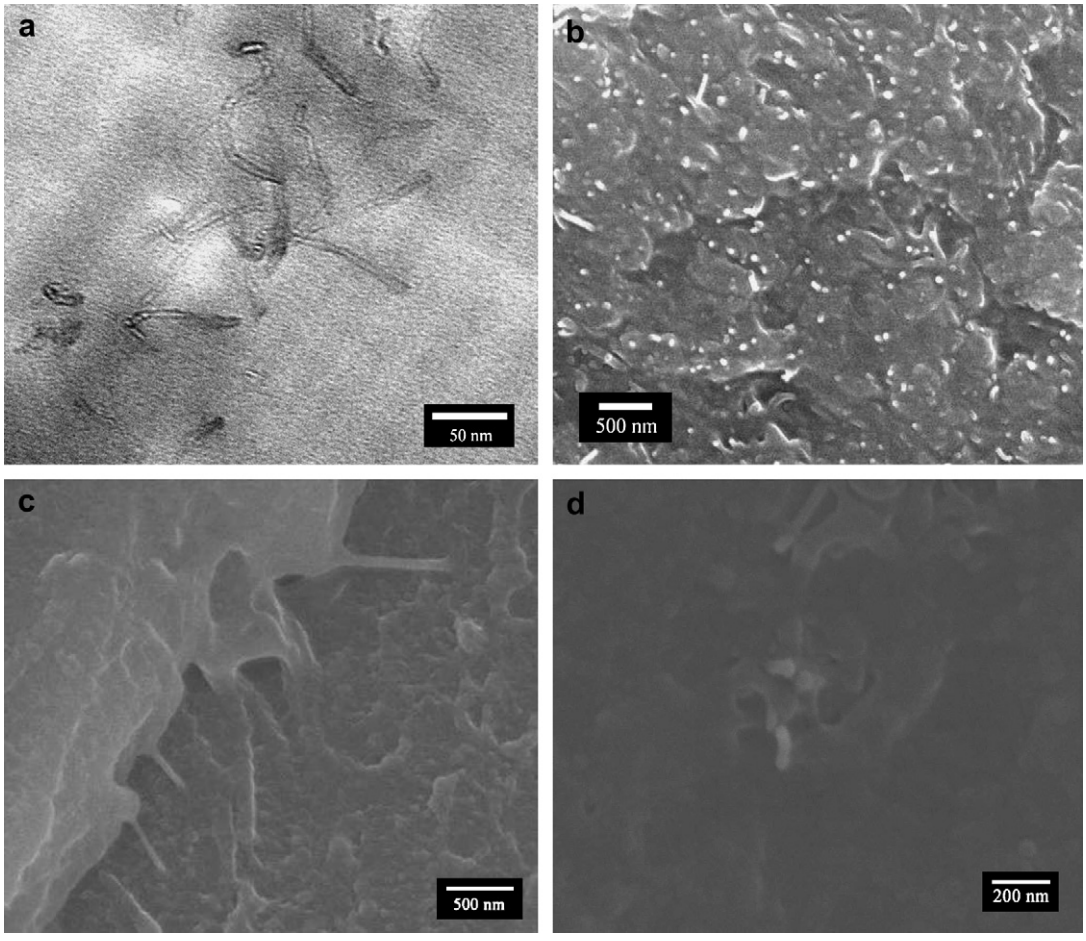

Fig. 12. Representative (a) TEM images of the PEN/m-CNT 0.1, (b) SEM images of the PEN/m-CNT 0.5, and (c) and (d) the fracture surfaces of the PEN/m-CNT 0.5 nanocomposites.

CNT stabilizes their dispersion by good interactions with the PEN matrix, resulting from the increased polarity by the functional groups formed on the surfaces of the m-CNT as well as good interactions of the –COOH groups with the C═O groups of the PEN matrix. This interfacial adhesion between the m-CNT and the PEN matrix is crucial for improving the mechanical properties of the PEN nanocomposites. The fractured surfaces of the PEN/m-CNT nanocomposites are also shown in Fig. 12(c) and (d). It can be seen that two ends of the m-CNT were covered by the PEN matrix, and this feature indicated that the m-CNT had a good wetting with the PEN matrix, suggesting the existence of strong interactions between them. The presence of the functional groups on the surfaces of the m-CNT resulted in the interfacial interaction between the polymer matrix and the nanotubes in the PEN/m-CNT nanocomposites. For instance, the hydrogen atoms at the –COOH groups of the m-CNT may form hydrogen bonding with the C═O groups of PEN macromolecular chains as shown in Scheme 1. Meng and coworkers [82] reported that for multi-walled CNT (MWCNT) and polyamide 6 (PA6) nanocomposites, acid-treated MWCNT was effectively dispersed in the PA6 matrix, because the functional groups on the surface of modified MWCNT probably have reacted with PA6 in melt-mixing process, resulting in better dispersion state and stronger interfacial adhesion. This result can be considered as the evidence for efficient load transfer between the PEN matrix and the m-CNT during the tensile testing.

3.5. Mechanical properties

The mechanical properties of pure PEN, the PEN/p-CNT, and the PEN/m-CNT nanocomposites are shown in Fig. 13. The incorporation of a very small quantity of CNT significantly improved the mechanical properties of PEN nanocomposites due to the nanoreinforcing effect of CNT with high aspect ratio. In comparison with pure PEN, the PEN nanocomposites exhibited higher tensile strength and tensile modulus, and this enhancing effect was more pronounced in the case of the PEN/m-CNT nanocomposites. On the incorporation of 0.5 wt% of the m-CNT, the tensile strength of the PEN/m-CNT nanocomposites was significantly improved by 32% from 66.3 to 87.8 MPa, and the tensile modulus was improved by 18% from 1.68 to 1.98 GPa, relative to PEN matrix. The enhancement of the mechanical properties of the PEN/m-CNT nanocomposites was attributed to the better interfacial bonding between the m-CNT and the PEN matrix as well as the better dispersion of the m-CNT in the PEN matrix. The incorporation of the m-CNT containing C–C bond defects and –COOH groups into the PEN matrix resulted in the good interfacial adhesion between the m-CNT and the PEN matrix, suggesting that the functional groups formed on the surfaces of the m-CNT were helpful for improving the interfacial interaction with C═O groups in the PEN matrix, thus being favorable to more effective load transfer from the polymer matrix to the nanotubes. Therefore, the enhancement of the homogeneous dispersion and the interfacial adhesion in the PEN/m-CNT nanocomposites, resulting from strong interactions between the m-CNT and the PEN chains, can lead to the significant improvement in the overall mechanical properties of the PEN/m-CNT nanocomposites. As shown in Table 2, the elongation at break for the PEN nanocomposites was decreased with the introduction of p-CNT and m-CNT, indicating that the PEN nanocomposites became somewhat brittle as compared to pure PEN because of the increased stiffness of the PEN nanocomposites and the micro-voids formed around the nanotubes during the tensile testing. However, PEN/m-CNT nanocomposites exhibited higher value of the elongation at break than that of PEN/p-CNT, which was attributed to the enhancement of the homogeneous dispersion of m-CNT and the interfacial interactions between m-CNT and PEN matrix. Similar observation has been reported that modified CNT-filled PA6 nanocomposites had higher tensile strength and elongation at break than unmodified CNT-filled PA6 nanocomposites due to high dispersion state and strong interfacial adhesion and that the incorporation of acid-treated CNT also restricted the motion of PA6 chains physically or chemically, thus the elongation at break of modified CNT/PA6 nanocomposites was less than that of pure PA6 [82].

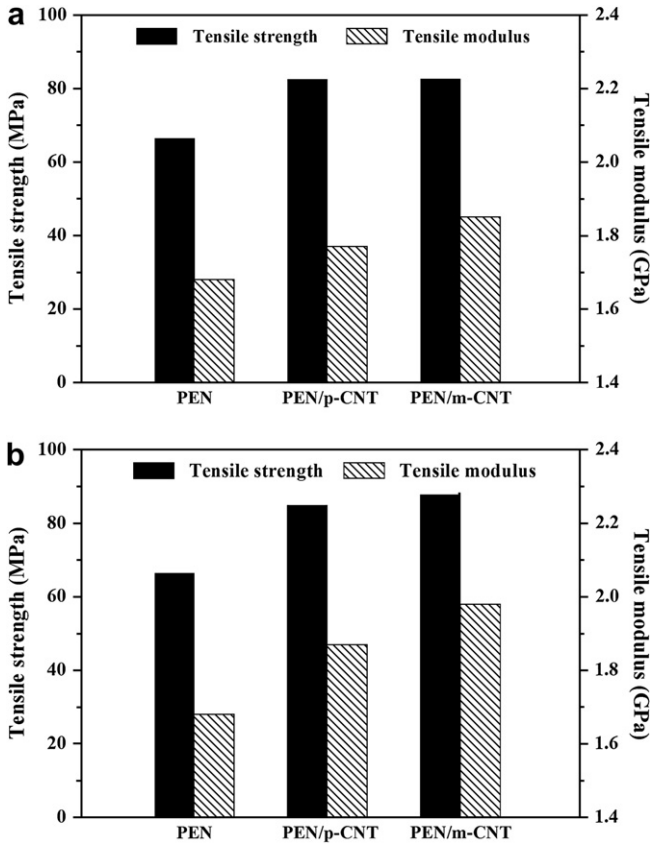

Fig. 13. Mechanical properties of PEN nanocomposites containing (a) 0.1 and (b) 0.5 wt% of CNT content.

For characterizing the effect of the CNT on the mechanical properties of the PEN nanocomposites, it is also instructive to compare the experimental results with the values predicted from the theoretical models. It is known that the modified Halpin–Tsai equation has been used to predict the modulus of the CNT-filled polymer nanocomposites [83,84]. Assuming the random oriented discontinuous distribution of the m-CNT in the PEN matrix, the modified Halpin–Tsai equation can be expressed as follows [83–86]:

$$E_C = \left[\left(\frac{3}{8}\right)\left(\frac{1+2(l_{CNT}/d_{CNT})\eta_L V_{CNT}}{1-\eta_L V_{CNT}}\right) + \left(\frac{5}{8}\right)\left(\frac{1+2\eta_T V_{CNT}}{1-\eta_T V_{CNT}}\right)\right]E_{PEN} \quad \text{where } \eta_L = \frac{(E_{CNT}/E_{PEN})-1}{(E_{CNT}/E_{PEN})+2(l_{CNT}/d_{CNT})}\ \eta_T = \frac{(E_{CNT}/E_{PEN})-1}{(E_{CNT}/E_{PEN})+2} \quad (2)$$

Table 2
The mechanical properties of the PEN nanocomposites

Materials	Tensile strength (MPa)	Tensile modulus (GPa)	Elongation at break (%)
PEN	66.3 ± 4.8	1.68 ± 0.032	253.2 ± 24
PEN/p-CNT 0.5	84.9 ± 3.6	1.87 ± 0.025	126.4 ± 20
PEN/m-CNT 0.5	87.8 ± 3.4	1.98 ± 0.021	145.8 ± 21

where E_C, E_{PEN}, and E_{CNT} are the tensile modulus of the nanocomposites, the PEN, and the CNT, respectively; l_{CNT}/d_{CNT} is the ratio of length to diameter for the CNT, and V_{CNT} is the volume fraction of the CNT in the nanocomposites. To fit Eq. (2) to the experimental results for the PEN nanocomposites, the weight fraction was transformed to the volume fraction, taking the densities of the PEN (1.407 g/cm^3) [87] and the perfectly graphitized CNT (2.16 g/cm^3) [83,84]. The theoretical values of the nanocomposite modulus can be estimated assuming the aspect ratio of ~1000 and E_{CNT} of ~450 GPa. The E_{CNT} values used in this study represent a mid-range value in the modulus ranges of the CNT previously measured [88].

The tensile strength of the PEN/m-CNT nanocomposites can be estimated from the following equation [89]:

$$\sigma_C = \sigma_{CNT} V_{CNT} + \sigma_{PEN} V_{PEN} \quad (3)$$

where σ_C, σ_{CNT}, and σ_{PEN} are the tensile strength of the nanocomposites, the CNT, and the PEN, respectively. The theoretical values of the nanocomposite strength can be estimated based on the sCNT value that is ~11 GPa based on previous literature [90].

The theoretically predicted values and the experimental data for the modulus and the strength of the PEN/m-CNT nanocomposites are compared in Fig. 14. The experimental results for the mechanical properties of the PEN nanocomposites were lower than those of theoretically predicted values. At lower m-CNT content, the PEN/m-CNT nanocomposites exhibited higher values than those of theoretically predicted values. This result suggested that the interfacial interaction was more effective in the enhancement of the mechanical properties of the PEN nanocomposites at 0.1 wt% of CNT content than at 0.5 wt% of CNT content. Similar effect has been also observed in the MWCNT grafted polyhedral oligomeric silsequioxane (MWCNT-*g*-POSS) and poly(L-lactide) (PLLA) nanocomposite systems [22] in that for MWCNT-*g*-POSS/PLLA nanocomposites, the interfacial interactions were more effective in strengthening the nanocomposites at low MWCNT-*g*-POSS loading than at high MWCNT-*g*-POSS loading. Therefore, the synergistic effect of the combined strong interfacial interaction and homogenous dispersion was more effective at lower CNT content for improving the mechanical properties of the PEN nanocomposites. In summary, the introduction of the m-CNT into the PEN matrix resulted in the improvement in the interfacial adhesion between the m-CNT and the PEN as well as the good dispersion of the m-CNT, thereby enhancing significantly the overall mechanical properties of the PEN/m-CNT nanocomposites.

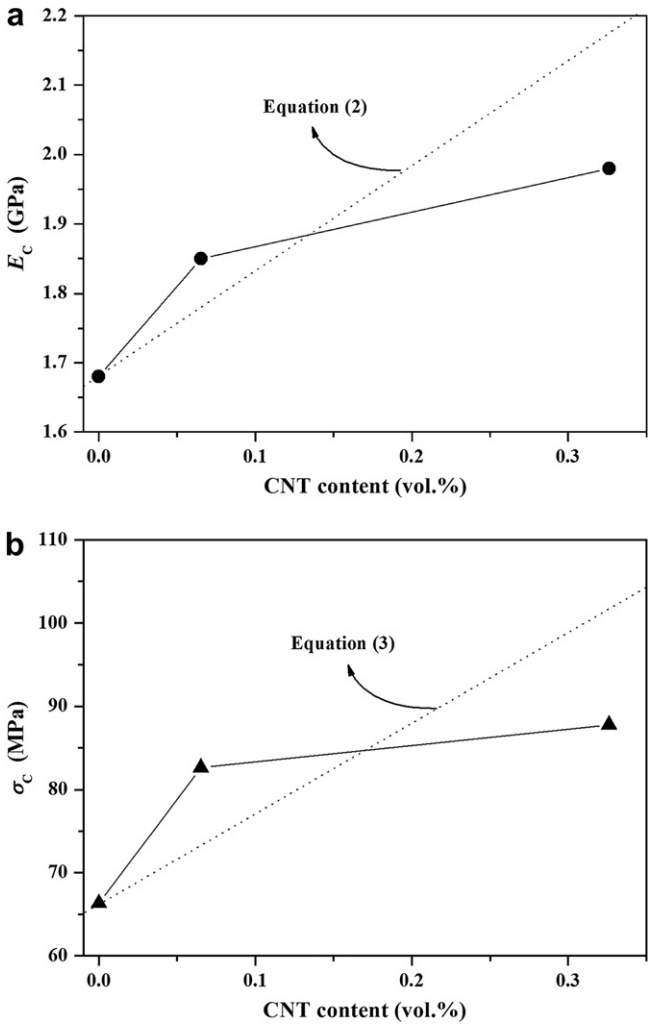

Fig. 14. Theoretically predicted values and the experimental results for (a) the composite modulus and (b) the composite strength of the PEN/m-CNT nanocomposites (dotted lines represent the theoretically predicted values).

4. Conclusions

Aromatic polyester nanocomposites based on the PEN and the CNT for improving the dispersion and the interfacial adhesion were prepared by a direct melt blending in a twin-screw extruder. The chemical modification of the CNT appeared to facilitate the dispersion state of the CNT in the PEN matrix and the interfacial adhesion between them. The activation energy for thermal decomposition of the PEN nanocomposites reflected that the incorporation of very small quantity of the CNT into the PEN matrix enhanced the thermal stability of the PEN nanocomposites and this enhancing effect was more pronounced in the case of the PEN/modified CNT (m-CNT) nanocomposite. The morphological observation demonstrated that uniform dispersion of the m-CNT and strong interfacial adhesion or intimate contact between the nanotubes and the polymer matrix can lead to the efficient load transfer from the PEN matrix to the nanotubes, resulting in significant enhancement of the mechanical properties of the PEN/m-CNT nanocomposite even with the introduction of very small quantity of the m-CNT. For the CNT-reinforced PEN nanocomposites, strong interfacial adhesion and uniform dispersion are more crucial factors for improving the physical properties of the nanocomposites.

References

[1] Iijima S. Nature 1991;354:56.
[2] Liu C, Fan YY, Liu M, Cong HT, Cheng HM, Dresselhaus MS. Science 1999;286:1127.
[3] Ishihara T, Kawahara A, Nishiguchi H, Yoshio M, Takita Y. J Power Sources 2001;97–98:129.
[4] Wu M, Shaw L. Int J Hydrogen Energy 2005;30:373.
[5] De Heer WA, Chatelain A, Ugarte D. Science 1995;270:1179.
[6] Fan S, Chapline MG, Franklin NR, Tombler TW, Casell AM, Dai H. Science 1999;283:512.
[7] Kim P, Lieber CM. Science 1999;286:2148.
[8] Kong J, Franklin N, Zhou C, Peng S, Cho JJ, Dai H. Science 2000;287:622.
[9] Alan B, Dalton AB, Collins S, Muñoz E, Razal JM, Ebron VH, et al. Nature 2003;423:703.
[10] Ebbesen TW. Annu Rev Mater Sci 1994;24:235.
[11] Dresselhaus MS, Dresselhaus G, Avouris PH. Carbon nanotubes: synthesis, structure, properties, and applications. Berlin: Springer; 2001.
[12] Bokobza L. Polymer 2007;48:5279.
[13] Kim JY, Kim SH. J Polym Sci Part B Polym Phys 2005;43:3600.
[14] Kim JY, Kim SH. Polym Int 2006;55:449.
[15] Kim JY, Kim OS, Kim SH, Jeon HY. Polym Eng Sci 2004;44:395.
[16] Kim JY, Kang SW, Kim SH. Fibers Polym 2006;7:358.
[17] Kim JY, Kim SH. J Appl Polym Sci 2006;99:2211.
[18] Kim JY, Kim SH, Kikutani T. J Polym Sci Part B Polym Phys 2004;42:395.
[19] Kim JY, Seo ES, Kim SH, Kikutani T. Macromol Res 2003;11:62.
[20] Kim JY, Kim SH, Kang SW, Chang JH, Ahn SH. Macromol Res 2006;14:146.
[21] Kim JY, Kang SW, Kim SH, Kim BC, Shim KB, Lee JG. Macromol Res 2005;13:19.

[22] Chen GX, Shimizu H. Polymer 2008;49:943.
[23] Choi JY, Han SW, Huh WS, Tan LS, Baek JB. Polymer 2007;48:4034.
[24] Song W, Zheng Z, Tang W, Wang X. Polymer 2007;48:3658.
[25] Ebbesen T. Carbon nanotubes: preparation and properties. New York: CRC Press; 1997.
[26] Lourie O, Cox DM, Wagner HD. Phys Rev Lett 1998;81:1638.
[27] Shaffer MSP, Windle AH. Adv Mater 1999;11:937.
[28] Gong X, Liu J, baskara S, Voise RD, Young JS. Chem Mater 2000;12:1049.
[29] Liu J, Rinzler AG, Dai H, Hafner JH, Bradley RK, Boul PJ, et al. Science 1998;280:1253.
[30] Sun YP, Fu K, Lin Y, Huang W. Acc Chem Res 2002;35:1096.
[31] Hirsch A. Angew Chem Int Ed 2002;41:11.
[32] Cui S, Canet R, Derre A, Couzi M, Delhaes P. Carbon 2003;41:797.
[33] Bellayer S, Gilman JW, Eidelman N, Bourbigot S, Flambard X, Fox DM, et al. Adv Funct Mater 2005;15:910.
[34] Haggenmuller R, Conmas HH, Rinzler AG, Fischer JE, Winey KI. Chem Phys Lett 2000;330:219.
[35] Jia ZJ, Wang ZY, Liang J, Wei BQ, Wu DH. Mater Sci Eng A 1999;271:395.
[36] Jin JX, Pramoda KP, Goh SH, Xu GQ. Mater Res Bull 2002;37:271.
[37] Pöschke P, Fornes TD, Paul DR. Polymer 2002;43:3247.
[38] Jung R, Park WI, Kwon SM, Kim HS, Jin HJ. Polymer 2008;49:2071.
[39] Mu M, Walker AM, Torkelson JM, Winey KI. Polymer 2008;49:1332.
[40] Pegel S, Pöschke P, Petzold G, Alig I, Dudkin SM, Lellinger D. Polymer 2008;49:974.
[41] Kim JY, Park HS, Kim SH. J Appl Polym Sci 2007;103:1450.
[42] Kim JY, Han SI, Kim SH. Polym Eng Sci 2007;47:1715.
[43] Kim JY, Kim SH. J Polym Sci Part B Polym Phys 2006;44:1062.
[44] Kim JY, Park HS, Kim SH. Polymer 2006;47:1379.
[45] Tzavalas S, Drakonakis V, Mouzakis DE, Fischer D, Gregoriou G. Macromolecules 2006;39:9150.
[46] Zhu J, Peng H, Rodriguez-Macias F, Margrave JL, Khabashesku VN, Imam AM, et al. Adv Funct Mater 2004;14:643.
[47] Mawhinney DB, Naumenko V, Kuznetsova A. J Am Chem Soc 2000;122:2383.
[48] Eitan A, Jiang K, Dukes D, Andrews R, Schadler LS. Chem Mater 2003;15:3198.
[49] Yuang Y, Young RJ. J Mater Sci 1994;29:4027.
[50] Ruan SL, Gao P, Yang XG, Yu TX. Polymer 2003;44:5643.
[51] Tuinstra E, Koening JI. J Chem Phys 1970;53:1126.
[52] Baibarac M, Baltog I, Lefrant S, Gomez-Romero P. Polymer 2007;48:5279.
[53] Grossiord N, Loss J, Regev O, Koning CE. Chem Mater 2006;18:1089.
[54] Hu H, Yu A, Kim E, Zhao B, Itkis ME, Bekyarova E, et al. J Phys Chem B 2005;109:11520.
[55] Cai H, Yan FY, Xue QJ. Mater Sci Eng A 2004;364:94.
[56] Zhao LP, Gao L. Carbon 2004;42:423.
[57] Jung DD, Bhattacharyya D, Easteal AJ. J Polym Sci Part B Polym Phys 2001;82:1504.
[58] Gupta MC, Umare SS. Macromolecules 1992;25:138.
[59] Watts PCP, Mureau N, Tang Z, Miyajima Y, Carey JD, Silva SRP. Nanotechnology 2007;18:175701.
[60] Tseng CH, Wang CC, Chen CY. Chem Mater 2007;19:308.
[61] Horowitz HH, Metzger G. Anal Chem 1963;35:1464.
[62] Lee HK, Pejanovic S, Mondragon I, Mijovic J. Polymer 2007;48:7345.
[63] Benedict LX, Lourie SG, Cohen ML. Solid State Commun 1996;100:177.
[64] Berber S, Kwon YK, Tomanek D. Phys Rev Lett 2000;84:4614.
[65] Wu CS, Liao HT. Polymer 2007;48:4449.
[66] Xu D, Wang Z. Polymer 2008;49:330.
[67] Li L, Li CY, Ni C, Rong L, Hsiao B. Polymer 2007;48:3452.
[68] Abdalla M, Derrick D, Adibempe D, Nyairo E, Robinson P, Thompson G. Polymer 2007;48:5662.
[69] Abdel-Goad M, Pötschke P. J Non-Newtonian Fluid Mech 2005;128:2.
[70] Pinnavaia TJ, Beall GW. Polymer–clay nanocomposites. New York: Wiley; 2000 [chapters 6–7].
[71] Wagner R, Reisinger TJG. Polymer 2003;44:7513.
[72] Enikolopyan NS, Fridman ML, Stalnova IU, Popov VL. Adv Polym Sci 1990;96:1.
[73] Krishnamoorti R, Vaia RA, Giannelis EP. Chem Mater 1996;8:1728.
[74] Ferry J. Viscoelastic properties of polymers. New York: Wiley; 1980.
[75] Krisnamoorti R, Giannelis EP. Macromolecules 1997;30:4097.
[76] Rosedalev JH, Bates FS. Macromolecules 1990;23:2329.
[77] Larson RG, Winey KI, Patel SS, Watanabe H, Bruinsma R. Rheol Acta 1993;32:245.
[78] Van Gulp M, Palmen J. Rheol Bull 1998;67:5.
[79] Trinkle S, Friedrich C. Rheol Acta 2002;41:103.
[80] Honerkamp J, Weese J. Rheol Acta 1993;32:57.
[81] Han CD, Kim J, Kim JK. Macromolecules 1989;22:383.
[82] Meng H, Sui GX, Fang PF, Yang R. Polymer 2008;49:610.
[83] Qian D, Dickey EC, Andrew R, Rantall T. Appl Phys Lett 2000;76:2868.
[84] Cadek M, Coleman JN, Barron V, Hedicke K, Blau WJ. Appl Phys Lett 2002;81:5123.
[85] Mallick PK. Fiber-reinforced composites. New York: Marcel Dekker; 1993.
[86] Zhang X, Liu T, Sreekumar TV, Kumar S, Moore VC, Hauge RH, et al. Nano Lett 2003;3:1285.
[87] Ito M, Kikutani T. In: Fakirov S, editor. Handbook of thermoplastic polyesters. Weinheim: Wiley-VCH; 2002 [chapter 10].
[88] Pan ZW, Xie SS, Lu L, Chang BH, Sun LF, Zhou WY, et al. Appl Phys Lett 1999;74:3152.
[89] Agarwal BD, Broutman LG. Analysis and performance of fiber composites. New York: Wiley; 1980.
[90] Yu MF, Lourie O, Dyer MJ, Moloni K, Kelly TF, Ruoff RS. Science 2000;287:637.